

TWO-PHASE CLOSED THERMOSYPHON WITH NANOFLUIDS

Balkrishna Mehta and Sameer Khandekar

Department of Mechanical Engineering

Indian Institute of Technology Kanpur

Kanpur 208016 India.

Tel: +91-512-2597038, Fax: +91-512-259-7408, E-mail: samkhan@iitk.ac.in

ABSTRACT

Nanofluids, stabilized suspensions of nanoparticles typically < 100 nm in conventional fluids, are evolving as potential enhanced heat transfer fluids due to their better thermal conductivity, increase in single phase heat transfer coefficient and significant increase in critical boiling heat flux. In the present paper, we investigate the overall thermal resistance of a closed two-phase thermosyphon using pure water and various water based nanofluids (of Al_2O_3 , CuO and Laponite clay) as working fluids. We observed that all these nanofluids show inferior thermal performance than pure water. Furthermore, it is observed that the wettability of all nanofluids on copper substrate, having the same average roughness as that of the thermosyphon container pipe, is better than that of pure water. The behavior of nanofluids is explained in the light of pool boiling dynamics and the interplay of nucleating cavities with wettability of the nanofluids.

KEY WORDS: Nanofluids, Pool boiling, Two-phase Closed Thermosyphon, Wettability.

1. INTRODUCTION

The present scenario of high thermal loading coupled with high flux levels demands exploration of new heat transfer augmentation mechanisms. In this context, 'Nanofluids' may emerge as alternative heat transfer fluids. The term 'Nanofluids' is used to indicate a special class of heat transfer fluids that contain nanoparticles ($< \sim 100$ nm) of metallic/non metallic substances uniformly and stably suspended in a conventional coolant [1]. This opens the possibility of enhancing/tailoring the thermophysical properties of the base fluid in a desired manner. The idea of suspending some solid phase material in conventional liquids to enhance its heat transfer properties is not new; the main problems with such systems are: (a) wear/clogging of pumps, heat exchangers, (b) phase separation, agglomeration. Nanoparticles can remain in suspension almost indefinitely in nanofluids, despite substantial difference in their respective bulk densities. Moreover, recent studies indicate that nano-particles can favorably alter thermophysical or transport properties of the base fluid. In this background, the present work aims to study the thermal performance of closed two-phase gravity thermosyphons with nanofluids.

After the introductory concept by Choi et al [1], subsequent studies in the last decade have indicated that nanofluids exhibit [2]:

- (i) Enhanced thermal conductivities as compared to conventional solid-liquid suspensions
- (ii) Strongly non-linear temperature dependent effective thermal conductivity
- (iii) An increase (some reports indicating decrease) in single-phase heat transfer coefficient
- (iv) A decrease (some reports indicating increase) in pool boiling heat transfer coefficient
- (v) An increase in pool boiling CHF

The literature also suggests that the observed behavior of nanofluids is, in many cases, anomalous to predictions of the existing macroscopic theories. Since thermophysical properties of the working fluid play a vital role in quantifying heat transfer rates, nanofluids have given an impetus to the idea of developing tailor made fluids best suited for a given application. In principle therefore, a fluid with 'better' thermophysical properties may be engineered. Which thermophysical properties need to be altered by addition of nanoparticles has to be addressed in the light of the mechanisms that govern the device performance characteristics.

2. DESIGN OF EXPERIMENT

Gravity thermosyphons are designed so as not to exceed the heat throughput, under the following limitations: (i) dry-out limitation (ii) Counter Current Flow Limitation (CCFL) or flooding, and (iii) Boiling Limitation (BL).

In the present proposed experiments since the FR was always 100%, dry-out limitation was not a relevant consideration. The CCFL is the most important and common limitations found in closed two-phase thermosyphons. The generally accepted CCFL correlation is [3]:

$$\hat{Ku}_{CCFL} = \frac{(Q_{max} / A_{axi})}{h_{fg} \rho_v^{0.5} [g\sigma(\rho_l - \rho_v)]^{1/4}} \quad (1)$$

where

$$\hat{Ku}_{CCFL} = \tilde{K} \cdot [1 + (\rho_v / \rho_l)^{0.25}]^{-2} \quad (2)$$

$$\tilde{K} = (\rho_l / \rho_v)^{0.14} \cdot \tanh^2 Bo^{1/4} \quad (3)$$

$$Bo = d[g(\rho_l - \rho_v)/\sigma]^{1/2} \quad (4)$$

The BL is encountered in thermosyphons with large liquid fill ratios and high radial heat fluxes in the evaporator. In this limitation, vapor bubbles coalesce near the wall which prohibits the contact of liquid working fluid to wall surface resulting in rapid burn out. Golobič and Gašperšič [4] have compiled many CCFL/ BL correlations, one widely used being:

$$\hat{Ku}_{BL} = \frac{(Q_{max} / A_{rad})}{h_{fg} \rho_v^{0.5} [g\sigma(\rho_l - \rho_v)]^{1/4}} \quad (5)$$

where

$$\hat{Ku}_{BL} = 0.16 \left[1 - \exp\left\{(-d/L_e) \cdot (\rho_l / \rho_v)^{0.13}\right\} \right] \quad (6)$$

Comparing Eqs. (1) and (5) along with Eqs. (2) and (6), we note the following:

(i) Both Eqs. (1) and (5) are identical except the fact that the area of cross section of the thermosyphon ($A_{axi} = 0.25 \cdot \pi \cdot d^2$) is applicable in Eq. (1) while the radial evaporator area ($A_{rad} = \pi \cdot d \cdot L_e$) is considered in the latter. The denominator in both the equations is a direct manifestation of interface instability analysis coupled with dimensional analyses developed simultaneously by Kutateladze and Taylor, around the same time period [3].

(ii) It is seen from Eq. (2) that the parameter \tilde{K} takes into account the curvature effect of the

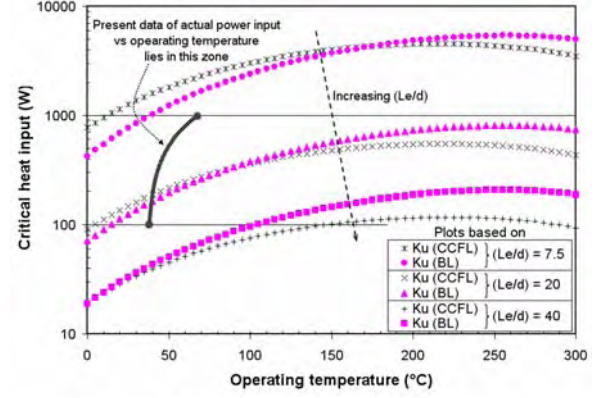


Figure 1: Effect of aspect ratio (L_e/d) on Kutateladze number (Ku) for different heat throughput limitation.

container in terms of the non-dimensional diameter, i.e. the Bond number. There is no explicit dependency on (L_e/d) in Eq. (2) as can be seen in Eq. (6). Previous studies show that for (L_e/d) > 60, CCFL predominates and when (L_e/d) ≤ 3-5, pool boiling characteristics has the predominant influence in limiting heat throughput. In the intermediate (L_e/d) range, it is difficult to explicitly differentiate between the two limitations [3, 5].

The above discussed aspects of the limitations can be seen clearly in Figure 1, where the maximum possible heat throughput, based on CCFL condition (Eq. 1, 2) and BL condition (Eq. 5, 6), is plotted. It is observed that in the operating range on 30°C - 70°C, BL predominates for low aspect ratios (L_e/d) while CCFL dominates at higher aspect ratios. Moreover, we can clearly distinguish the difference between BL and CCFL at lower (L_e/d). As this ratio increases respective critical heat fluxes tend to overlap with each other, thereby making it difficult to distinguish which phenomenon is responsible for the eventual burnout of evaporator wall, CCFL or BL.

In the present study, we chose an aspect ratio of 7.5 with $L_e = 120$ mm and $d = 16$ mm so as to render the device limited exclusively under BL, at least from theoretical considerations as discussed above. This design was chosen in the wake of recent studies, as mentioned earlier, that nanofluids have shown higher CHF in pool boiling conditions. The set-up allowed heat input from 0-1200 W. For a given experimental run, condenser cooling water was maintained at a specific temperature level, and the heat input to

the evaporator was slowly increased till the desired steady state operating temperature was obtained. The adiabatic operating temperatures ranged from 40°C to 65°C. Externally controlled conditions were kept identical for baseline experiments with pure water and those with nanofluids (Figure 1 highlights the actual range of conditions in which the present experiments were conducted). Thus, the thermosyphon always operated under ‘normal’ operating conditions and its performance in terms of net thermal resistance could be ascertained, as reported in the present work¹.

3. DESCRIPTION OF SETUP

The details of the set-up, along with relevant dimensions, are shown in Figure 2. Heat was supplied to the evaporator by the copper heating block (120 X 50 X 50 mm) having a central bore to accommodate the thermosyphon tube. Four mica insulated surface heaters (116 X 48 mm) were mounted on the outer surface of the block with the help of a stainless steel backing plate. Finned tube condenser (40 square fins of 70 X 70 X 1 mm size at a pitch of 6.5 mm) was made for the heat removal from the thermosyphon. Cross flow conditions existed over the condenser fins on the shell side. A cryostat bath (Haake® DC10K20) was used to circulate the cooling water (always maintained at 30°C) to the condenser. Eight K-Type thermo-couples were used to measure the temperature at axial locations on the thermosyphon tube as shown in Figure 2. PC based data acquisition was done by a high precision DAQ. Before proceeding to test nanofluids, baseline experiments were conducted with degassed/ deionized water. Once the integrity, quality and repeatability of the baseline data was established, then three water based nanofluids (1% of nanoparticle by weight respectively in all cases) were used as the working fluids, viz. CuO (8.6 to 13.5 nm), Al₂O₃ (40-47 nm) and Laponite clay (discs of radius 25 nm, thickness 1 nm). All nanoparticles were procured from established commercial vendors. Laponite (Na^{+0.7}[(Si₈Mg_{5.5}Li_{0.3})O₂₀(OH)₄]^{-0.7}) is a colloidal synthetic layered silicate; the sol forming variant of laponite has been used in this study.

¹ The determination of limiting behavior under critical boiling heat flux conditions necessitated upgraded control of the condenser conditions so as to maintain cooling water at isothermal conditions. Since this was not available, CHF behavior of nanofluids in thermosyphons is not reported.

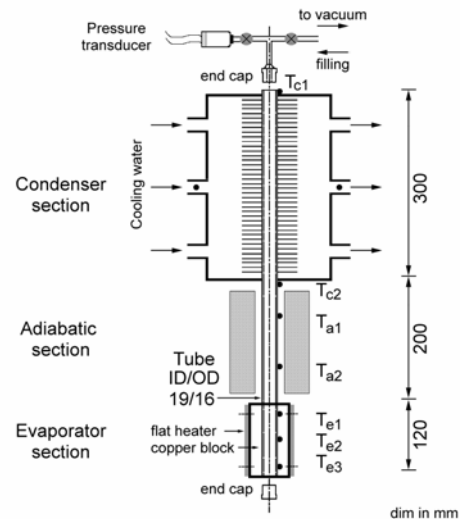


Figure 2: Schematic of the thermosyphon experimental setup.

Thorough cleaning of the device is vital for the success of the experiment and data reliability/repeatability. Changeover from one nanofluid to the other must be preceded by a reliable cleaning protocol to ensure that there are no remnants of the earlier sample inside the device. This was achieved by three cycle operation of cleaning/rinsing with deionized water, acetone and ethanol and vacuum drying. This was followed by another cycle in which the device was placed inside an ultra-sonicator with continuous rinsing with water. Finally, the tube was cured under vacuum for extended time period. This procedure was followed with every changeover of the working fluid. In between the changeover, the device was first tested with deionized/degassed water to repeatedly generate baseline data for thermal resistance.

4. RESULTS AND DISCUSSION

Figure 3 shows the comparative observation of thermal resistance of thermosyphon with pure water and different nanofluids, where,

$$R_{th} = (T_e - T_c) / Q_{in} \quad (7)$$

where, T_e and T_c are average values of the respective thermocouples placed locally (refer Figure 2). All nanofluids reduce the thermal performance with varying degrees. To understand this phenomenon we need to focus our attention on essentially two aspects:

- (a) Effect of nanoparticles on pool boiling characteristics in the evaporator.
- (b) Effect of nanoparticles on condensation heat transfer characteristics.

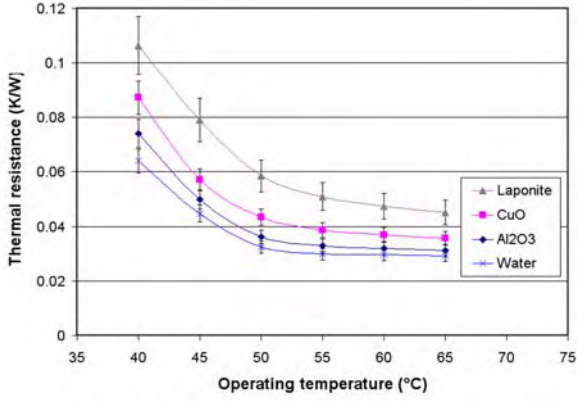


Figure 3: Thermal resistance of the thermosyphon with different nanofluids as compared to pure water.

The condenser section needs scrutiny only under the hypothetical premise that nanoparticles are transported upwards in that zone by the vapor inertia. There is no conclusive evidence to support this hypothesis at this stage, but the fact that even micron sized pollutant particulates do not settle down for extended periods in the atmosphere strongly indicates that the possibility of nanoparticle transport in the condenser section cannot be ruled out. This issue needs to be addressed separately.

In this paper, we will concentrate the discussion on the effect of nanoparticles on pool boiling dynamics in the evaporator. Literature suggests that there is an enhancement in single-phase heat transfer coefficient with nanofluids. While under laminar flow conditions, the heat transfer coefficient is a linear function of the fluid thermal conductivity, in turbulent flows, the classical Dittus-Boelter correlation suggests that:

$$h_{\text{conv}} \propto \left[\frac{C_p}{\mu_1} \right]^{2/5} \cdot [k_1]^{3/5} \quad (8)$$

Thus, for turbulent case also, single-phase convective heat transfer increases with thermal conductivity of the base fluid. Thus, the increase in the thermal conductivity of base fluid due to addition of nano-particles can possibly explain the corresponding increase in heat transfer coefficient.

Under pool boiling conditions, as literature suggests, so also in the present experimental results, there is indeed a reduction in heat transfer coefficient. Looking at this trend, in the wake of

the contrasting increase in single phase heat transfer coefficient and the classical Rohsenow/Froster-Zuber correlations for pool boiling [6], which are based on single-phase convection analogy, the following conclusions can be drawn:

(a) During nucleate pool boiling, the single-phase convective transport is patently affected by many complementary effects such as bubble departure diameter and frequency, nucleation site density and the average rise velocity of individual bubbles. The impact of these parameters on pool boiling heat transfer is definitely getting adversely affected by the nanoparticles. The adverse effect is stronger than the complementary increase in single-phase heat transfer coefficient brought solely by the increased thermal conductivity of the nanofluid. The fact that there is an unequivocal degradation of thermal performance under nucleate pool boiling regime indicates the need to study the interplay between the suspended nanoparticles with the heater wall surface².

(b) Practically all models describing nucleate boiling heat transfer suggest a power law dependence of nucleate boiling heat flux on the nucleation site density and the wall superheat [7]:

$$q'' = (n'_a)^x \cdot (T_w - T_{\text{sat}})^y \quad (9)$$

Various classical models suggest different values of exponents x , y ; in general, for most models, x varies between 0.3 and 0.5 while y varies between 1.0 and 1.8. In case of nanofluids, the active nucleation site density n'_a can get affected by two mechanisms:

(i) physical adhesion, blockage, gradual filling up of active nucleation sites with nanoparticles thereby reducing the cavity mouth radius, and increasing the cavity half angle

(ii) a change in contact angle/wetting characteristics if the base fluid with the heater surface due to the addition of nanoparticles.

² The bulk thermal conductivity of metal oxide nanoparticles (CuO = 32.6 W/m-K and Al₂O₃ = 40 W/m-K) is an order of magnitude higher than water whereas for Laponite the same is quite low (bulk Laponite = 0.15 W/m-K). While pool boiling heat transfer depends on the interaction and interplay of many parameters simultaneously (thermal conductivity of the fluid being one of them), the trend in the thermal performance of the thermosyphon, although it follows the trend in the bulk thermal conductivity of the used nanoparticles, cannot be fully attributed to this sole effect.

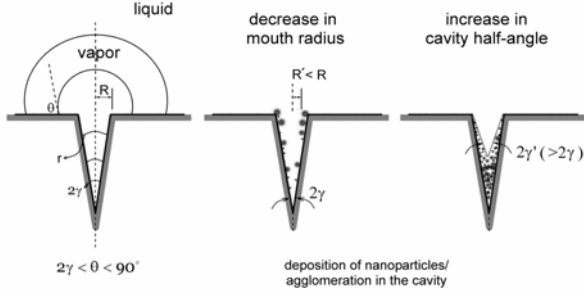


Figure 4: A nucleating cavity (left) and possible physical adhesion/clogging of nanoparticles in the cavities thereby affecting cavity mouth radius and half-angle.

Referring to Figure 4, if the cavity radius is denoted by R , and the minimum interface radius during embryo growth is denoted by r_{\min} , the condition for the cavity to be active can be stated as:

$$T_1 - T_{\text{sat}} > \frac{2 \cdot \sigma \cdot T_{\text{sat}} \cdot v_{\text{fg}}}{h_{\text{fg}} \cdot r_{\min}} \quad (10)$$

For situations where the contact angle θ is large and $R/r \leq 1$, r_{\min} can be approximated by R , Eq. (10) becomes:

$$T_1 - T_{\text{sat}} > \frac{2 \cdot \sigma \cdot T_{\text{sat}} \cdot v_{\text{fg}}}{h_{\text{fg}} \cdot R} \quad (11)$$

This equation clearly suggests that as the cavity mouth radius, R decreases (which may be due to physical adhesion, blockage etc., as suggested above), then a higher superheat is required to activate a given site. In the present study, the size of the nanoparticles is definitely less than the roughness value of the boiling surface³. Thus, it is quite likely that nanoparticles get entrapped in the nucleating surface cavities thereby reducing its size and degrading the active nucleation site density (as suggested in Figure 4). Also, it is expected that certain degree of agglomeration occurs in the nanoparticles during vapor generation inside the cavities. This will slowly lead to increased concentration of nanoparticles inside the cavity which will finally lead to its blockage and deactivation. Thus, deposition of nanoparticles due to sustained nucleation on a material surface may indeed degrade its surface quality so as to reduce the heat transfer coefficient.

³ The average roughness R_a of the boiling surface of the thermosiphon copper container was measured by a laser profilometer before the experiment and found to be 0.24 microns

For situations where $2\gamma < \theta < 90^\circ$ (this is true for the present case; Figure 4, 5), the minimum interface radius during embryo growth (r_{\min}) may not always equal to the cavity radius R , but may vary with the contact angle and cavity half angle γ . Such a function may be denoted as [6]:

$$\frac{r_{\min}}{R} = \Psi(\theta, \gamma) \quad (12)$$

This implies that for a given surface having cavities with specified γ , the associated value of r_{\min} may depend on the contact angle θ . Thus, Eq (10), reads:

$$T_1 - T_{\text{sat}} > \frac{2 \cdot \sigma \cdot T_{\text{sat}} \cdot v_{\text{fg}}}{h_{\text{fg}} \cdot R \cdot \Psi(\theta, \gamma)} \quad (13)$$

This equation clearly suggests the dependence of required superheat on the contact angle of the fluid (with the heater material) and the cavity half-angle. In Figure 4 we also postulated that because of accumulation and/or trapping of nanoparticle in the cavity (or the groove), the half-angle will tend to increase. Furthermore, in order to investigate effect of contact angle, static contact angles of sessile droplets of the two nanofluids were measured on flat copper substrate with the help of a goniometer. Figure 5 shows the main results along with experimental conditions. There is a marked difference in the contact angle of nanofluids as compared to pure water. It is clear from these tests that addition of nanoparticles strongly affects the wettability of the base fluid. The wettability of laponite nanofluid on copper substrate was indeed much better than both, alumina nanofluid and pure water⁴. The transfer of a nanoparticle in the liquid medium strongly affects the surface energy of the mixture.

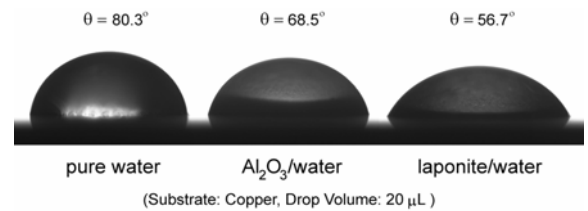


Figure 5: Images of sessile droplets of different fluids on copper substrate showing different contact angles.

⁴ CuO based nanofluid was difficult to stabilize as compared to the other two fluids. Therefore, contact angle data is not reported here; although, the wettability of this nanofluid also followed the general observed trend.

In the background of the fact that van der Waals forces are effective within about 100 nm range, the length scales of the nanoparticles definitely comes in the domain of influence of these forces [8]. Since the total surface free energy is the manifestation of interaction of different molecular forces (metallic bond, hydrogen bond, Keesom and Debye forces, London dispersion forces, Covalent bonds etc.), their effect on bulk thermophysical properties needs to be addressed while dealing with nanofluids. While the contact angle results of Figure 5 are under static conditions, they clearly indicate the trends obtained in the thermal performance of the thermosyphon vis-à-vis Eq. (13). Also, given the fact that CHF improves with wettability, the trends regarding CHF mechanisms with nanofluids can be partly explained. This aspect requires further investigations.

ACKNOWLEDGEMENTS

The work is partially funded by Department of Mechanical Engineering, IIT Kanpur, and Faculty Initiation Grant (N^o: #IITK/ME/20050019).

REFERENCES

1. Choi S. U. S., Enhancing thermal conductivity of fluids with nanoparticles, Developments and Applications of Non-Newtonian Flows, FED-Vol. 231/MD-Vol. 66, 1995, pp. 99–105.
2. Wang Xiang-Qi, Mujumdar A. S., Heat Transfer Characteristics of Nanofluids: A Review, Int. J. of Thermal Sciences, Vol. 46, 1–19, 2007
3. Faghri A., Heat Pipe Science and Technology, Taylor and Francis, 1995.
4. Golobič Iztok and Gašperšič Branko, Corresponding States Correlation for Maximum Heat Flux in Two-Phase Closed Thermosyphon, Int. J. Ref., Vol. 20, No. 6, pp. 402-410, 1997.
5. Groll M. and Rösler S., Operation Principles and Performance of Heat Pipes and Closed Two-Phase Thermosyphons, J. Non-Equilib. Thermo-dynamics, Vol. 17, pp. 91-151. 1992.
6. Carey Van P., Liquid-Vapor Phase Change Phenomena, 2nd Ed., Taylor & Francis, 2007.
7. Wallis G., One Dimensional Two-Phase Flow, McGraw-Hill Inc., 1969.
8. Israelachvili J., Intermolecular and Surface Forces, Academic Press, 2003.

NOMENCLATURE

A	: area of cross section (m ²)
C _p	: specific heat at constant pressure (J/kg·K)
d	: diameter of thermosyphon (m)
g	: acceleration due to gravity (m/s ²)
h	: heat transfer coefficient (W/m ² ·K)
h _{fg}	: latent heat of vaporization (J/kg)
k	: thermal conductivity (W/m·K)
L	: length (m)
n' _a	: active nucleation site density (m ⁻²)
\dot{Q}	: heat throughput rate (W)
R	: cavity mouth radius (m)
R _a	: average roughness (microns)
R _{th}	: thermal resistance (K/W or °C /W)
T	: temperature (°C or K)

Greek Symbols

σ	: surface tension (N/m)
ρ	: density (kg/m ³)
μ	: dynamic viscosity (N·s/m ²)
τ	: shear stress (N/m ²)
γ	: cavity half-angle (rad)
v _{fg}	: specific volume difference (m ³ /kg)

Subscripts

a	: adiabatic section
c	: condenser section
e	: evaporator section
f	: fluid
g	: gas/vapor
conv	: convective
crit	: critical
l	: liquid
o	: outer, outlet
sat	: saturation
v	: vapor

Abbreviations

BL	: Boiling Limitation
CCFL	: Counter Current Flow Limitation
FR	: Filling Ratio